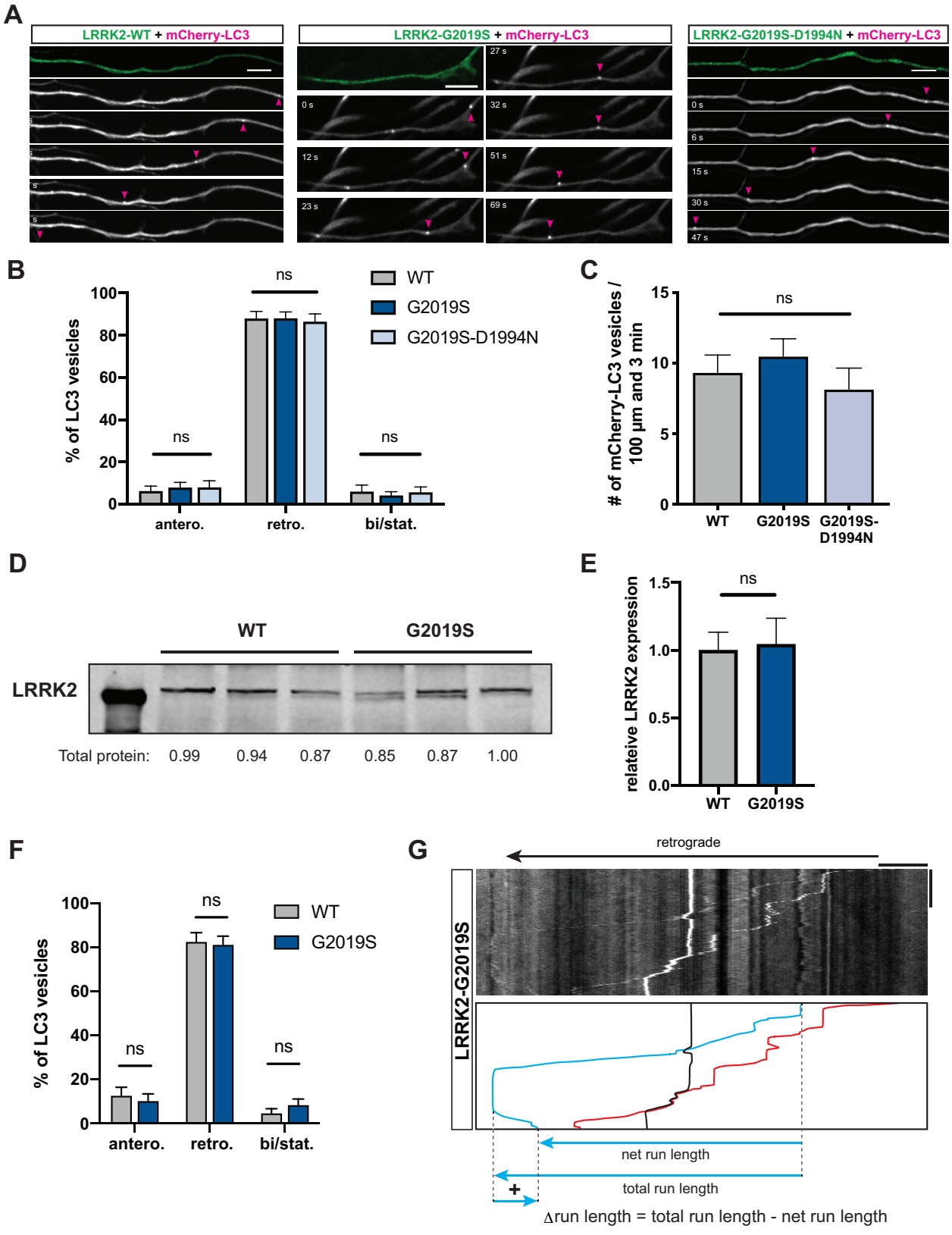
A
LRRK2-WT + mCherry-LC3
LRRK2-G2019S + mCherry-LC3
LRRK2-G2019S-D1994N + mCherry-LC3
0 s
6 s
15 s
30 s
47 s
27 s
32 s
12 s
51 s
23 s
69 s
B
% of LC3 vesicles
WT
G2019S
G2019S-D1994N
ns
antero.
retro.
bi/stat.
C
# of mCherry-LC3 vesicles / 100 µm and 3 min
WT
G2019S
G2019S-D1994N
D
LRRK2
WT
G2019S
Total protein: 0.99 0.94 0.87 0.85 0.87 1.00
E
relateive LRRK2 expression
F
% of LC3 vesicles
G
retrograde
LRRK2-G2019S
net run length
total run length
Δrun length = total run length - net run length

Figure S1. Overexpression or knock-in of LRRK2-G2019S does not affect density or transport directionality of axonal AVs. Related to Figure 1 and 2. (**A**) Time lapse images of axonal mCherry-LC3 vesicles in rat hippocampal neurons transfected with EGFP-LRRK2-WT, EGFP-LRRK2-G2019S, or EGFP-LRRK2-G2019S-D1994N. Arrowheads indicate the position of mCherry-LC3 vesicles at different time points. Scale bars, 5µm. (**B**) Directionality of AVs per axon in WT, G2019S, and G2019S-D1994N expressing neurons. Antero., anterograde; retro., retrograde; bi/stat., bidirectional/stationary (mean ± SEM; n = 17-20 neurons from 3 independent cultures; ns, not significant; Two-way ANOVA with Tukey's multiple comparisons test). (**C**) Number of mCherry-LC3 vesicles per 100 µm axonal length and 3 minutes imaging time in WT, G2019S, and G2019S-D1994N expressing neurons (mean ± SEM; n = 17-20 neurons from 3 independent cultures; ns, not significant, p=0.29; Kruskal-Wallis test). (**D**) Western Blot of LRRK2 in DIV8 WT or G2019S KI mouse cortical neurons. (**E**) Quantification of LRRK2 levels in DIV8 WT or G2019S KI mouse cortical neurons (mean ± SEM; n = 3 independent cultures; ns, not significant, p=0.86; Welch's t test). (**F**) Directionality of AVs per axon in WT and G2019S KI neurons. Antero., anterograde; retro., retrograde; bi/stat., bidirectional/stationary (mean ± SEM; n = 26 neurons from 3 independent cultures; ns, not significant; Two-way ANOVA with Sidak's multiple comparisons test). (**G**) Illustration of Δ run length quantification. Δ run length was calculated by subtracting the net run length from the total run length of each vesicle.

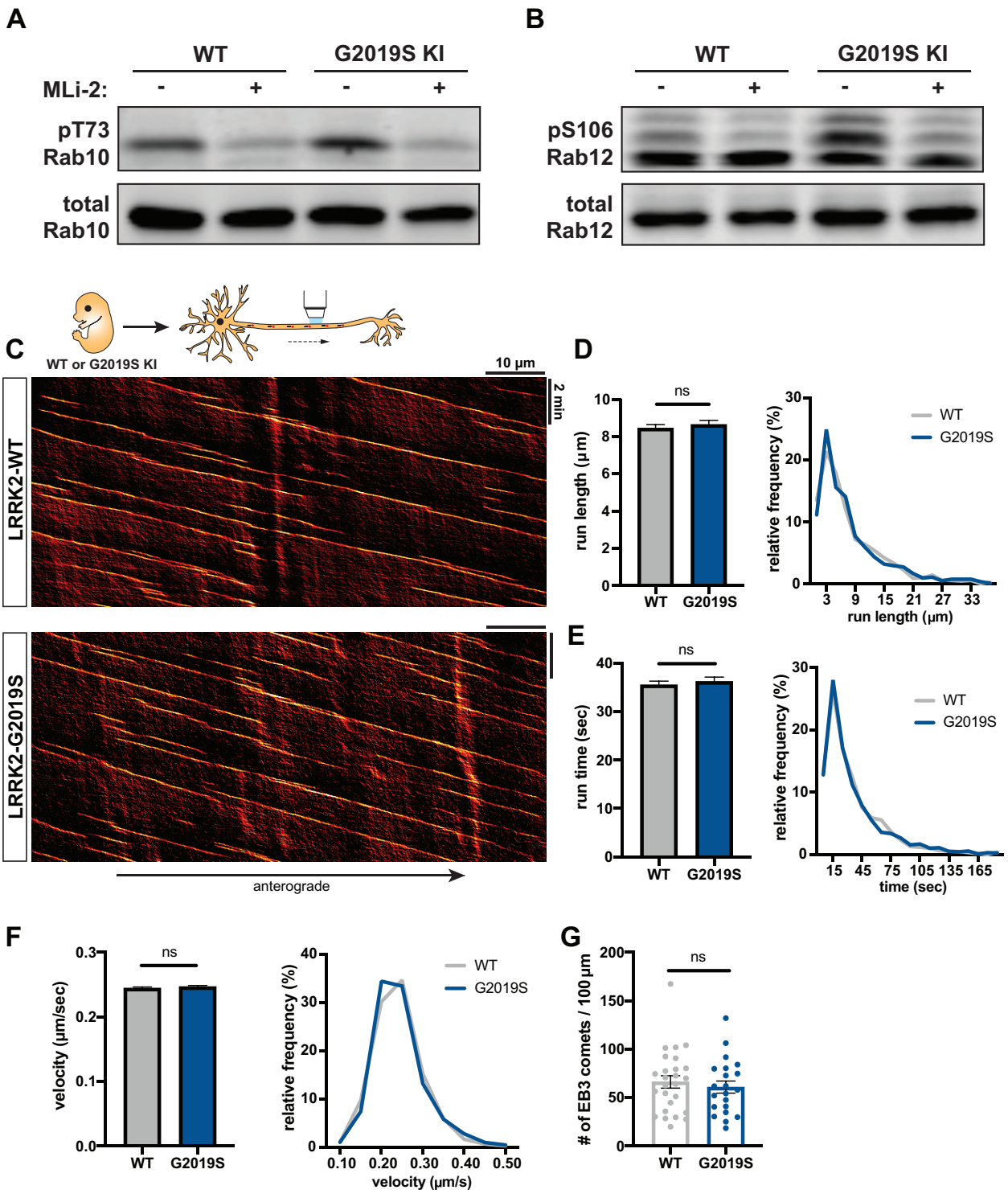
A
WT
G2019S KI
MLi-2:
-
+
-
+
pT73 Rab10
total Rab10
B
WT
G2019S KI
-
+
-
+
pS106 Rab12
total Rab12
C
WT or G2019S KI
10 µm
2 min
LRRK2-WT
LRRK2-G2019S
anterograde
D
ns
run length (µm)
WT
G2019S
relative frequency (%)
run length (µm)
E
ns
run time (sec)
WT
G2019S
relative frequency (%)
time (sec)
F
ns
velocity (µm/sec)
WT
G2019S
relative frequency (%)
velocity (µm/s)
G
ns
# of EB3 comets / 100 µm
WT
G2019S

Figure S2. LRRK2-G2019S knock-in does not affect axonal microtubule dynamics. Related to Figure 2. (**A**) Phospho T73 Rab10 Western blot of WT or G2019S KI neurons treated with DMSO or 100 nM MLi-2 overnight. (**B**) Phospho S106 Rab12 Western blot of WT or G2019S KI neurons treated with DMSO or 100 nM MLi-2 overnight. (**C**) Kymographs of axonal EB3-mCherry comets in WT and G2019S KI mouse cortical neurons. (**D**) Bar graph and frequency distribution of EB3 comet run length in WT and G2019S KI neurons (mean ± SEM; n = 1539-2009 comets from 21-26 neurons from 3 independent cultures; ns, not significant, p=0.96; Mann-Whitney test). Frequency distribution does not show run length > 38 μm (WT: 1.24%, G2019S: 1.56%). (**E**) Bar graph and frequency distribution of EB3 comet run time in WT and G2019S KI neurons (mean ± SEM; n = 1539-2009 comets from 21-26 neurons from 3 independent cultures; ns, not significant, p=0.80; Mann-Whitney test). Frequency distribution does not show run time > 190 sec (WT: 0.40%, G2019S: 0.52%). (**F**) Bar graph and frequency distribution of EB3 comet velocity in WT and G2019S KI neurons (mean ± SEM; n = 1539-2009 comets from 21-26 neurons from 3 independent cultures; ns, not significant, p=0.89; Mann-Whitney test). Frequency distribution does not show velocity > 0.55 μm/sec (WT: 0.75%, G2019S: 0.52%). (**G**) Number of EB3 comets per 100 μm axonal length and 10 minutes imaging time in WT and G2019S KI neurons (mean ± SEM; n = 21-26 neurons from 3 independent cultures; ns, not significant, p=0.55; Welch's t test).

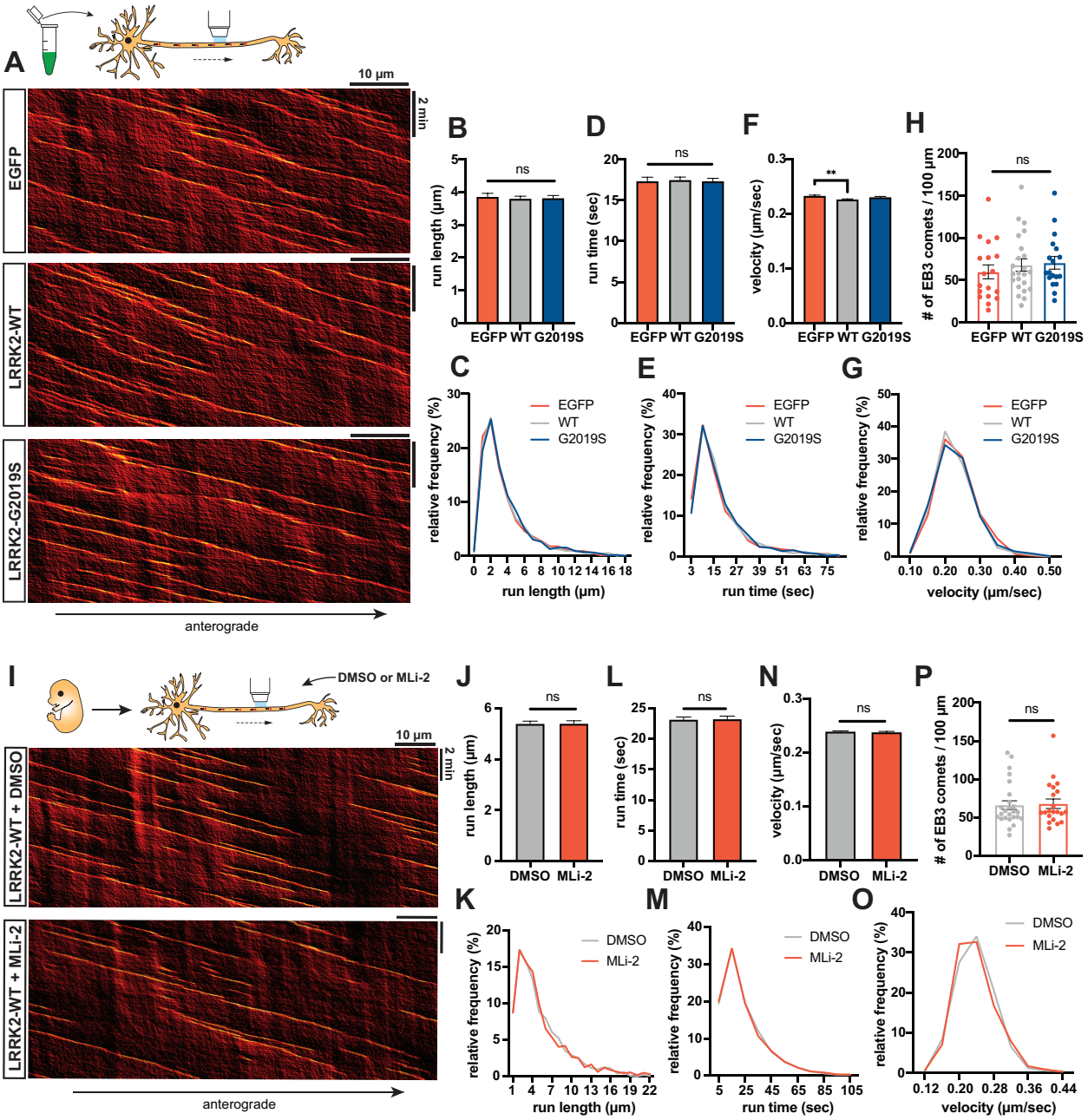
A
10 µm
2 min
EGFP
LRRK2-WT
LRRK2-G2019S
anterograde
B
run length (µm)
ns
EGFP WT G2019S
D
run time (sec)
ns
EGFP WT G2019S
F
velocity (µm/sec)
**
EGFP WT G2019S
H
# of EB3 comets / 100 µm
ns
EGFP WT G2019S
C
relative frequency (%)
EGFP
WT
G2019S
run length (µm)
E
relative frequency (%)
EGFP
WT
G2019S
run time (sec)
G
relative frequency (%)
EGFP
WT
G2019S
velocity (µm/sec)
I
DMSO or MLi-2
10 µm
2 min
LRRK2-WT + DMSO
LRRK2-WT + MLi-2
anterograde
J
run length (µm)
ns
DMSO MLi-2
L
run time (sec)
ns
DMSO MLi-2
N
velocity (µm/sec)
ns
DMSO MLi-2
P
# of EB3 comets / 100 µm
ns
DMSO MLi-2
K
relative frequency (%)
DMSO
MLi-2
run length (µm)
M
relative frequency (%)
DMSO
MLi-2
run time (sec)
O
relative frequency (%)
DMSO
MLi-2
velocity (µm/sec)

Figure S3. Neither LRRK2-G2019S overexpression nor treatment with MLi-2 affects axonal microtubule dynamics. Related to Figure 1 and 2. (**A**) Kymographs of axonal EB3-mCherry comets in rat hippocampal neurons expressing EGFP, EGFP-LRRK2-WT, or EGFP-LRRK2-G2019S. (**B**+**C**) Bar graph and frequency distribution of EB3 comet run length in EGFP, EGFP-LRRK2-WT, and EGFP-LRRK2-G2019S expressing neurons (mean ± SEM; n = 1186-1823 comets from 18-23 neurons from 3 independent cultures; ns, not significant p=0.52; Kruskal-Wallis test). Frequency distribution does not show run length > 18.5 µm (EGFP: 1.10%, WT: 0.77%, G2019S: 0.74%). (**D**+**E**) Bar graph and frequency distribution of EB3 comet run time in EGFP, EGFP-LRRK2-WT, and EGFP-LRRK2-G2019S expressing neurons (mean ± SEM; n = 1186-1823 comets from 18-23 neurons from 3 independent cultures; ns, not significant, p=0.11; Kruskal-Wallis test). Frequency distribution does not show run time > 84 sec (EGFP: 1.10%, WT: 0.88%, G2019S: 0.74%). (**F**+**G**) Bar graph and frequency distribution of EB3 comet velocity in EGFP, EGFP-LRRK2-WT, and EGFP-LRRK2-G2019S expressing neurons (mean ± SEM; n = 1186-1823 comets from 18-23 neurons from 3 independent cultures; **p=0.0021; Kruskal-Wallis with Dunn's multiple comparisons test). Frequency distribution does not show velocity > 0.5 µm/sec (EGFP: 0.17%, WT: 0.05%, G2019S: 0.13%). (**H**) Number of EB3 comets per 100 µm axonal length and 10 minutes imaging time in EGFP, EGFP-LRRK2-WT, and EGFP-LRRK2-G2019S expressing neurons (mean ± SEM; n = 18-23 neurons from 3 independent cultures; ns, not significant, p=0.61; One-way ANOVA). (**I**) Kymographs of axonal EB3-mCherry comets in WT mouse cortical neurons treated with DMSO or 100 nM MLi-2 overnight. (**J**+**K**) Bar graph and frequency distribution of EB3 comet run length in WT neurons treated with DMSO or MLi-2 (mean ± SEM; n = 1580-1836 comets from 21-25 neurons from 3 independent cultures; ns, not significant, p=0.77; Mann-Whitney test). Frequency distribution does not show run length > 22 µm (DMSO: 1.14%, MLi-2: 0.44%). (**L**+**M**) Bar graph and frequency distribution of EB3 comet run time in WT neurons treated with DMSO or MLi-2 (mean ± SEM; n = 1580-1836 comets from 21-

25 neurons from 3 independent cultures; ns, not significant, p=0.96; Mann-Whitney test). Frequency distribution does not show run time > 110 sec (DMSO: 0.49%, MLi-2: 0.32%). (**N**+**O**) Bar graph and frequency distribution of EB3 comet velocity in WT neurons treated with DMSO or MLi-2 (mean ± SEM; n = 1580-1836 comets from 21-25 neurons from 3 independent cultures; ns, not significant, p=0.14; Mann-Whitney test). Frequency distribution does not show velocity > 0.44 µm/sec (DMSO: 0.11%, MLi-2: 0.06%). (**P**) Number of EB3 comets per 100 µm axonal length and 10 minutes imaging time in WT neurons treated with DMSO or MLi-2 (mean ± SEM; n = 21-25 neurons from 3 independent cultures; ns, not significant, p=0.76; Mann-Whitney test).

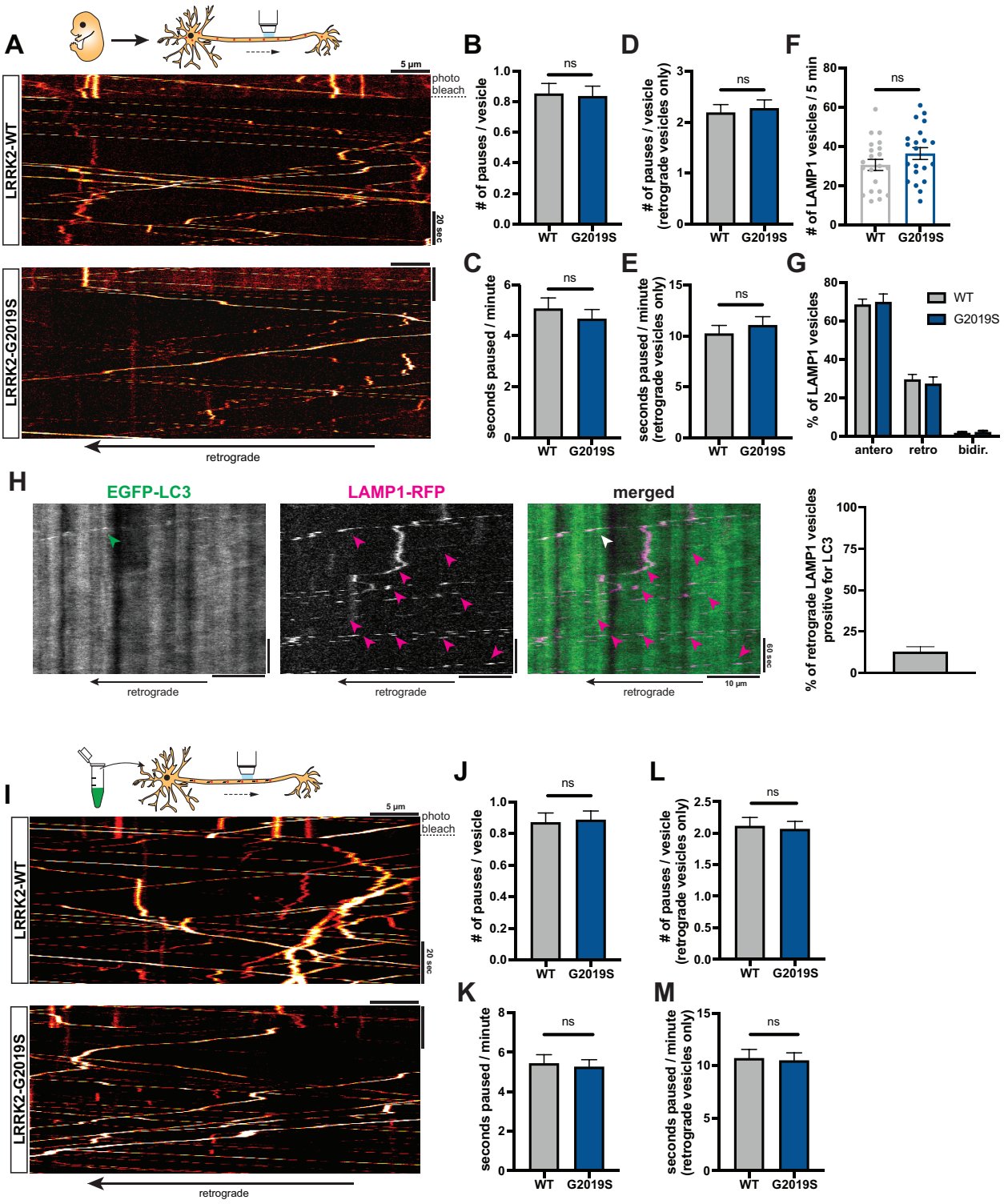
A
5 µm
photo bleach
LRRK2-WT
20 sec
LRRK2-G2019S
retrograde
B
# of pauses / vesicle
ns
WT
G2019S
C
seconds paused / minute
D
# of pauses / vesicle (retrograde vesicles only)
E
seconds paused / minute (retrograde vesicles only)
F
# of LAMP1 vesicles / 5 min
G
% of LAMP1 vesicles
antero
retro
bidir.
H
EGFP-LC3
LAMP1-RFP
merged
60 sec
10 µm
% of retrograde LAMP1 vesicles prositive for LC3
I
J
K
L
M

Figure S4. LRRK2-G2019S does not affect axonal transport of LAMP1 vesicles. Related to Figure 1 and 2. (**A**) Kymographs of axonal LAMP1-RFP vesicles in WT and G2019S KI mouse cortical neurons. The axon was photobleached to deplete the signal of stationary vesicles, aiding visualization of mobile vesicles and accurate quantification of pause events. (**B**) Pause number per LAMP1 vesicle in WT and G2019S KI neurons (mean ± SEM; n = 633-752 LAMP1 vesicles from 21 neurons from 3 independent cultures; ns, not significant, p=0.15; Mann-Whitney test). (**C**) Fraction of time paused (as measured by seconds paused per minute) of LAMP1 vesicles in WT and G2019S KI neurons (mean ± SEM; n = 633-752 LAMP1 vesicles from 21 neurons from 3 independent cultures; ns, not significant, p=0.13; Mann-Whitney test). (**D**) Pause number per retrograde LAMP1 vesicle in WT and G2019S KI neurons (mean ± SEM; n = 184-192 LAMP1 vesicles from 21 neurons from 3 independent cultures; ns, not significant, p=0.91; Mann-Whitney test). (**E**) Fraction of time paused of retrograde LAMP1 vesicles in WT and G2019S KI neurons (mean ± SEM; n = 184-192 LAMP1 vesicles from 21 neurons from 3 independent cultures; ns, not significant, p=0.82; Mann-Whitney test). (**F**) Number of LAMP1 vesicles entering the photobleached axonal area of interest within 5 minutes in WT and G2019S KI neurons (mean ± SEM; n = 21 neurons from 3 independent cultures; ns, not significant, p=0.17; Welch's t test). (**G**) Directionality of LAMP1 vesicles in WT or G2019S KI neurons. Note that the quantification only includes motile LAMP1 vesicles, as stationary vesicles were photobleached prior to image acquisition. Antero., anterograde; retro., retrograde; bidir., bidirectional (mean ± SEM; n = 21 neurons from 3 independent cultures; ns, not significant, p=0.95; Two-way ANOVA with Sidak's multiple comparisons test). (**H**) Representative kymographs and quantification of the fraction of retrograde LAMP1 vesicles positive for LC3 in the mid-axon of mouse cortical neurons (mean ± SEM; n = 26 neurons from 3 independent cultures). (**I**) Kymographs of axonal LAMP1-RFP vesicles in rat hippocampal neurons overexpressing EGFP-LRRK2-WT or EGFP-LRRK2-G2019S. Stationary LAMP1 vesicles were photobleached to aid visualization and accurate

quantification of pause events. (**J**) Pause number per LAMP1 vesicle in WT and G2019S expressing neurons (mean ± SEM; n = 626-761 LAMP1 vesicles from 18 neurons from 4 independent cultures; ns, not significant, p=0.87; Mann-Whitney test). (**K**) Fraction of time paused of LAMP1 vesicles in WT and G2019S expressing neurons (mean ± SEM; n = 626-761 LAMP1 vesicles from 18 neurons from 4 independent cultures; ns, not significant, p=0.91; Mann-Whitney test). (**L**) Pause number per retrograde LAMP1 vesicle in WT and G2019S expressing neurons (mean ± SEM; n = 183-251 LAMP1 vesicles from 18 neurons from 4 independent cultures; ns, not significant, p=0.72; Mann-Whitney test). (**M**) Fraction of time paused of retrograde LAMP1 vesicles in WT and G2019S expressing neurons (mean ± SEM; n = 183-251 LAMP1 vesicles from 18 neurons from 4 independent cultures; ns, not significant, p=0.76; Mann-Whitney test).

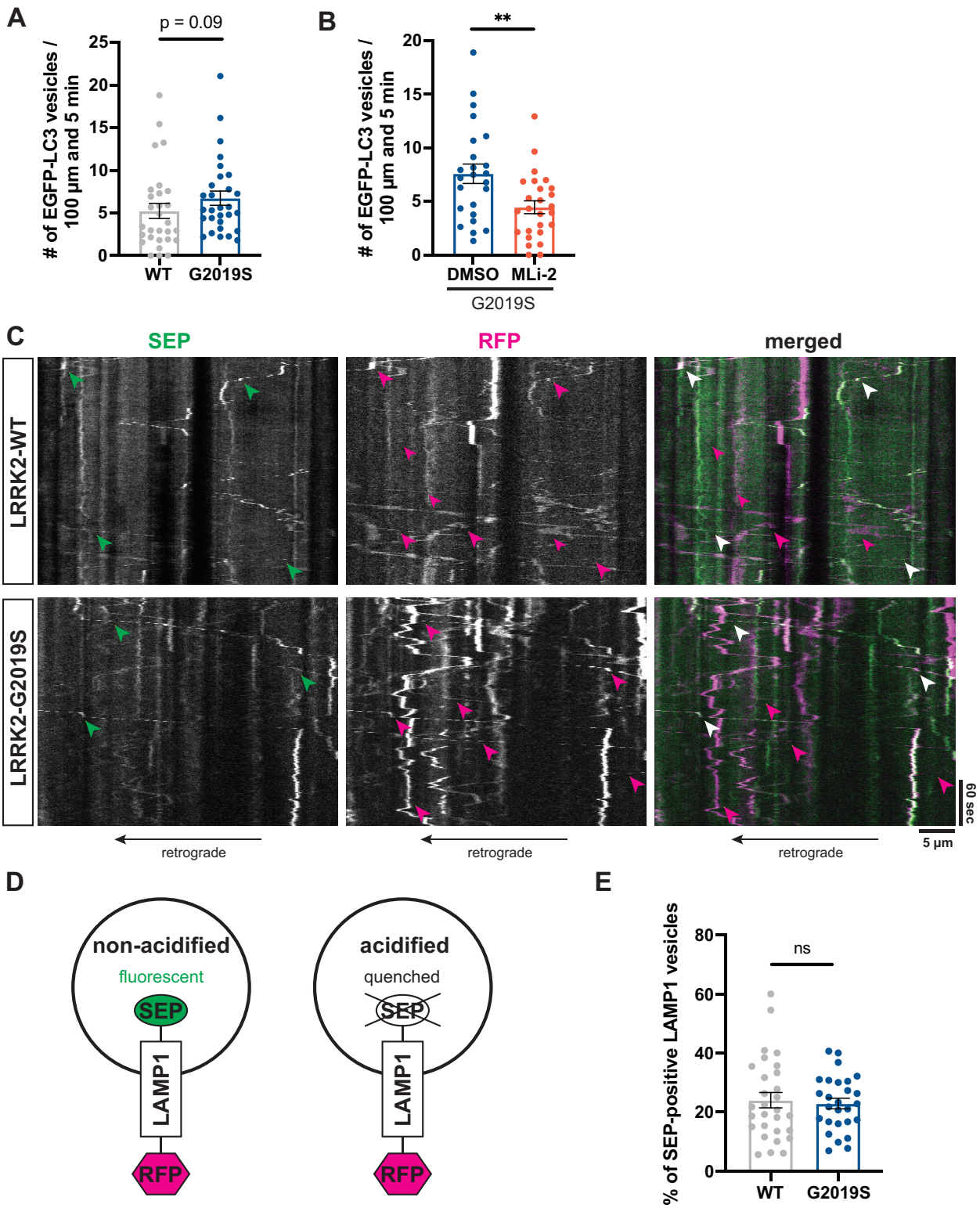
A
p = 0.09
# of EGFP-LC3 vesicles / 100 µm and 5 min
25
20
15
10
5
0
WT
G2019S
B
**
# of EGFP-LC3 vesicles / 100 µm and 5 min
20
15
10
5
0
DMSO
MLi-2
G2019S
C
SEP
RFP
merged
LRRK2-WT
LRRK2-G2019S
60 sec
5 µm
retrograde
retrograde
retrograde
D
non-acidified
fluorescent
SEP
LAMP1
RFP
acidified
quenched
SEP
LAMP1
RFP
E
ns
% of SEP-positive LAMP1 vesicles
80
60
40
20
0
WT
G2019S

Figure S5. LRRK2-G2019S affects the number of LC3 vesicles in the proximal axon but does not affect acidification of axonal LAMP1 vesicles. Related to Figure 4. (**A**) Number of EGFP-LC3 vesicles per 100 µm and 5 minutes imaging time in the proximal axon of WT and G2019S KI mouse cortical neurons (mean ± SEM; n = 29 neurons from 4 independent cultures; p=0.091; Mann-Whitney test). (**B**) Number of EGFP-LC3 vesicles per 100 µm and 5 minutes imaging time in the proximal axon of G2019S KI mouse cortical neurons treated overnight with DMSO or 100 nM MLi-2 (mean ± SEM; n = 24-26 neurons from 3 independent cultures; **, p=0.0066; Welch's t test). (**C**) Kymographs of SEP-LAMP1-RFP vesicles in the mid-axon of WT or G2019S KI mouse cortical neurons. Green arrowheads: SEP-positive traces; magenta arrowheads: RFP-positive traces; white arrowheads: SEP- and RFP-positive traces. (**D**) Schematic of SEP-LAMP1-RFP construct. SEP signal is quenched upon acidification, so acidified LAMP1 vesicles are labeled by RFP only. (**E**) Percentage of SEP-positive (= non-acidified) axonal LAMP1 vesicles in WT and G2019S KI neurons (mean ± SEM; n = 27-29 neurons from 3 independent cultures; ns, not significant, p=0.72; Welch's t test).

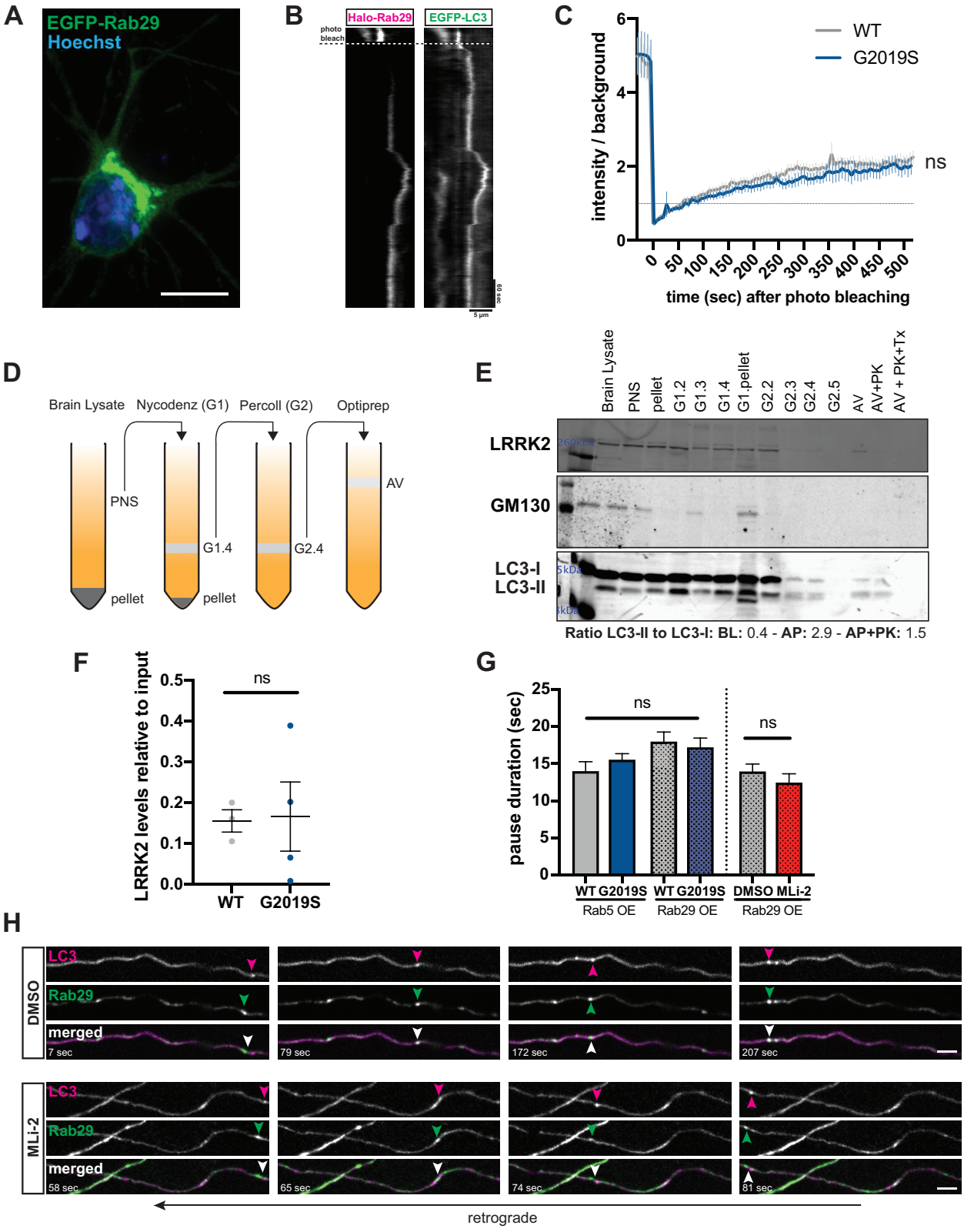
A
EGFP-Rab29
Hoechst
B
Halo-Rab29
EGFP-LC3
photo bleach
C
WT
G2019S
intensity / background
time (sec) after photo bleaching
ns
D
Brain Lysate
Nycodenz (G1)
Percoll (G2)
Optiprep
PNS
G1.4
G2.4
AV
pellet
pellet
E
Brain Lysate
PNS
pellet
G1.2
G1.3
G1.4
G1.pellet
G2.2
G2.3
G2.4
G2.5
AV
AV+PK
AV + PK+Tx
LRRK2
GM130
LC3-I
LC3-II
Ratio LC3-II to LC3-I: BL: 0.4 - AP: 2.9 - AP+PK: 1.5
F
LRRK2 levels relative to input
ns
WT
G2019S
G
pause duration (sec)
ns
ns
WT G2019S
Rab5 OE
WT G2019S
Rab29 OE
DMSO MLi-2
Rab29 OE
H
DMSO
LC3
Rab29
merged
7 sec
79 sec
172 sec
207 sec
MLi-2
LC3
Rab29
merged
58 sec
65 sec
74 sec
81 sec
retrograde

Figure S6. Rab29 and LRRK2 are located on the outer AV membrane. Related to Figure 5. (**A**) Golgi-like distribution of EGFP-Rab29 in the neuronal soma. Scale bar, 10 µm. (**B**) Kymograph of the axonal AV shown in Figure 5B, illustrating fluorescence recovery after Halo-Rab29 photobleaching. (**C**) Quantification of fluorescence recovery after photobleaching Halo-Rab29 signal of axonal EGFP-LC3 labeled AVs (mean ± SEM; n = 22-26 neurons from 3 independent cultures; ns, not significant, p=0.42; Mixed-effect analysis). (**D**) Schematic of AV isolation assay from mouse brain lysates. PNS, postnuclear supernatant. (**E**) Western Blot of LRRK2, LC3 and GM130 from brain lysate and different fractions of the autophagosome isolation protocol. PNS, postnuclear supernatant; Prot. K, Proteinase K; Tx, Triton X-100. (**F**) Western Blot quantification of LRRK2 levels in autophagosome fraction of WT and G2019S KI mice. Data shown are normalized to total protein and relative to whole brain lysate (mean ± SEM; n = 3-4 biological replicates; ns, not significant; Kruskal Wallis test). (**G**) Pause duration during AV transport in WT and G2019S KI neurons overexpressing Rab5 or Rab29, and in Rab29 overexpressing WT neurons treated with DMSO or MLi-2 (Overexpression of Rab5 or Rab29 in WT and G2019S KI neurons: mean ± SEM; n = 107-149 AVs from 27-38 neurons from 3-4 independent cultures; ns, not significant, p>0.06; Kruskal-Wallis with Dunn's multiple comparisons test. Treatment of Rab29 overexpressing WT neurons with DMSO or MLi-2: mean ± SEM; n = 78-109 AVs from 26-27 neurons from 3 independent cultures; ns, not significant, p=0.19; Mann-Whitney test). (**H**) Time lapse images of mCherry-LC3 and EGFP-Rab29 vesicles in WT mouse cortical neurons treated with DMSO or 100 nM MLi-2 overnight. Arrowheads point to EGFP-Rab29 positive AVs. Scale bar, 5 µm

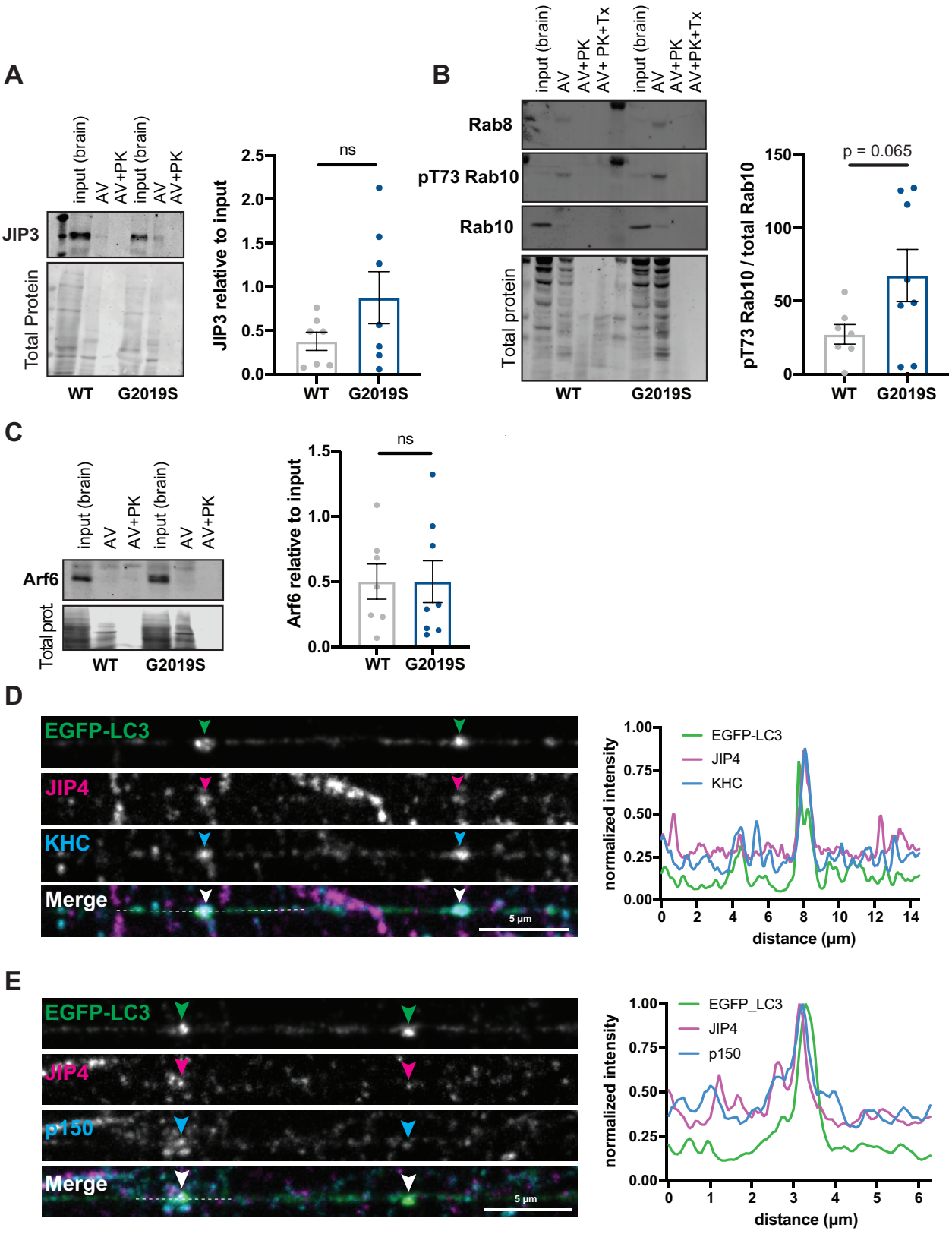
A
input (brain)
AV
AV+PK
input (brain)
AV
AV+PK
JIP3
Total Protein
WT
G2019S
JIP3 relative to input
ns
2.5
2.0
1.5
1.0
0.5
0.0
WT
G2019S
B
input (brain)
AV
AV+PK
AV+ PK+Tx
input (brain)
AV
AV+PK
AV+PK+Tx
Rab8
pT73 Rab10
Rab10
Total protein
WT
G2019S
pT73 Rab10 / total Rab10
p = 0.065
150
100
50
0
WT
G2019S
C
input (brain)
AV
AV+PK
input (brain)
AV
AV+PK
Arf6
Total prot
WT
G2019S
Arf6 relative to input
ns
1.5
1.0
0.5
0.0
WT
G2019S
D
EGFP-LC3
JIP4
KHC
Merge
5 µm
normalized intensity
1.00
0.75
0.50
0.25
0.00
EGFP-LC3
JIP4
KHC
0
2
4
6
8
10
12
14
distance (µm)
E
EGFP-LC3
JIP4
p150
Merge
5 µm
normalized intensity
1.00
0.75
0.50
0.25
0.00
EGFP_LC3
JIP4
p150
0
1
2
3
4
5
6
distance (µm)

Figure S7. LRRK2-G2019S recruits JIP4 to the autophagosome membrane. Related to Figure 6. (**A**) Representative Western Blot and quantification of JIP3 levels in the autophagosome fraction of WT and G2019S mouse brain lysates. Data shown are normalized to total protein and relative to whole brain lysate (mean ± SEM; n = 7 biological replicates; ns, not significant, p=0.1561; Welch's t test). (**B**) Representative Western Blot of total Rab8, pT73 Rab10, and total Rab10 levels in the autophagosome fraction of WT and G2019S mouse brain lysates. Total protein stain is the same as shown in Figure 6B (blots are from the same sample). Quantification of pT73 Rab10 normalized to total Rab10 in the autophagosome fraction of WT and G2019S mouse brain lysates (mean ± SEM; n = 7-8 biological replicates; ns, not significant, p=0.065; Welch's t test). (**C**) Western Blot and quantification of Arf6 levels in the autophagosome fraction of WT and G2019S mouse brain lysates. Data shown are normalized to total protein and relative to whole brain lysate (mean ± SEM; n = 7-8 biological replicates; ns, not significant, p=0.995; Welch's t test). (**D**) Maximum intensity projection and line scan of a G2019S KI neurite expressing EGFP-LC3 and stained for JIP4 (magenta) and KHC (blue). Dashed line indicates location of the line scan. Arrowheads highlight colocalization. (**E**) Maximum intensity projection and line scan of a G2019S KI neurite expressing EGFP-LC3 and stained for JIP4 (magenta) and p150 (blue). Dashed line indicates location of the line scan. Arrowheads highlight colocalization.